fraction precipitated from the antiserum with ammonium sulfate.
12. J. F. M. Leeuwenberg *et al.*, *J. Immunol.* **134**, 3770 (1985); H. Spits, H. Yssel, J. Leeuwenberg, J. E. DeVries, *Eur. J. Immunol.* **15**, 88 (1985).
13. D. M. Kranz, personal communication; H. Takayama *et al.*, *J. Immunol.* **138**, 566 (1987); S. C. Meuer *et al.*, *J. Exp. Med.* **158**, 988 (1983).
14. H. B. Fleit, S. D. Wright, J. C. Unkeless, *Proc. Natl. Acad. Sci. U.S.A.* **79**, 3275 (1982).
15. S. C. Meuer *et al.*, *ibid.* **81**, 1509 (1984); T. J. Henkel *et al.*, *J. Immunol.* **138**, 1221 (1987).
16. The $F(ab')_2$ fragment of anti-CD3 12F6 was prepared by diluting the antibody to 1.35 mg/ml in 0.1*M* acetate buffer, *p*H 4.1 [P. Parham, in *Immunochemistry*, D. M. Weir, L. A. Herzenberg, C. Blackwell, L. A. Herzenberg, Eds. (Blackwell, Oxford, 1986), pp. 14.11 and 14.14]; 175 μl of pepsin (1 mg/ml of pepsin in 0.1*M* acetate buffer, *p*H 4.1) was added and the mixture was digested at 37°C for 19.5 hours. The reaction was stopped by adding 3*M* tris-HCl, *p*H 8.6, to bring the *p*H above 7. The reaction mixture was then passed over a protein A–Sepharose 4B column, and the material not retained [$F(ab')_2$ fraction] was dialyzed against phosphate-buffered saline, *p*H 7.4; before use in chromium-51 release assays, it was ultracentrifuged at >100,000*g* to remove aggregates. The same extinction coefficient (1.4 mg^{-1} ml) was used for the $F(ab')_2$ fragments and intact antibody. The purified $F(ab')_2$ contained no remaining intact immunoglobulin visible by silver staining [C. R. Merril, D. Goldman, S. A. Sedman, M. H. Ebert, *Science* **211**, 1437 (1981)] a 7.5 percent polyacrylamide gel that had been overloaded with the purified $F(ab')_2$.
17. The differences in adhesiveness of various melanoma sublines to certain tissues appears to be correlated with variations in the morphology, motility, and metastatic potential of the melanoma cells [P. A. Netland and B. R. Zetter, *J. Cell Biol.* **101**, 720 (1985)]. B16F10 and M1313 differ markedly in their morphology (B16F10 being more cuboidal and M1313 spindle-shaped). It is possible that the difference in their susceptibility to lysis by anti-CD3 (unconjugated) and CTLs might be related to differences in expression of adhesion molecules, enabling the CTLs to bind M1313 cells to a greater degree than B16F10 cells.
18. L. Shen *et al.*, *J. Immunol.* **137**, 3378 (1986); B. Karpovsky, J. A. Titus, D. A. Stephany, D. M. Segal, *J. Exp. Med.* **160**, 1686 (1984).
19. We thank G. Matsueda for the synthesis of the cysteine-modified MSHa, R. Granstein for the human melanoma line B16F10, R. Bringhurst for the human melanoma line M1313, J. Kurnick for CTL clone 6B7, J. Unkeless for anti-FcR, Damon Biotech for anti-CD3 produced from hybridoma cells provided by R. Colvin, Biogen Research Corporation for rIL-2, and A. Hicks for help in preparing this manuscript. This work was supported by Cancer Center Core grant CA14051, by PHS grants CA28900, CA25472, and CA42504, and by Physician Scientist award AI00679 from the National Institutes of Health (to M.A.L.).

10 September 1987; accepted 11 December 1987

The Cellular *src* Gene Product Regulates Junctional Cell-to-Cell Communication

R. AZARNIA, S. REDDY, T. E. KMIECIK, D. SHALLOWAY, W. R. LOEWENSTEIN

Overexpression of the cellular *src* gene in NIH 3T3 cells causes reduction of cell-to-cell transmission of molecules in the 400- to 700-dalton range. This down-regulation of gap junctional communication correlates with the activity of the gene product, the protein tyrosine kinase $pp60^{c\text{-}src}$. The down-regulation was enhanced by point mutation of Tyr^{527} (a site that is phosphorylated in $pp60^{c\text{-}src}$ and that inhibits kinase activity) or by substitution of the viral-*src* for the cellular-*src* carboxyl-terminal coding region. Mutation of Tyr^{416} (a site phosphorylated upon Tyr^{527} mutation) suppresses both the down-regulation of communication by Tyr^{527} mutation and that by gene overexpression. The regulation of communication by *src* may be important in the control of embryonic development and cellular growth.

THE CELLULAR *src* GENE (c-*src*) (*1*) encodes the membrane-bound protein tyrosine kinase, $pp60^{c\text{-}src}$ (*2*). The gene is present in all species and is highly conserved. Its functions are still unknown. We have explored the possibility of a function in junctional communication, prompted by the finding that this communication is reduced by polyomavirus middle T antigen (*3*). This antigen binds to $pp60^{c\text{-}src}$, enhancing the protein tyrosine kinase activity of $pp60^{c\text{-}src}$ (*4*). We now report that junctional communication is reduced when the level of $pp60^{c\text{-}src}$ is elevated by incorporating c-*src* expression plasmids into mammalian cells, and that this action is enhanced by modifications in the carboxyl-terminal region of $pp60^{c\text{-}src}$, which increase transforming activity.

Our expression vectors contained the chicken c-*src* coding sequences ligated to retroviral long terminal repeats which provided promoter-enhancer sequences and polyadenylation sites (Fig. 1). Mouse NIH 3T3 cells were transfected with these plasmids, and cell lines were cloned from foci (suffix *foc*) or coselected for expression of *Eco-gpt* (suffix *cos*) or *neo* (*5*). The $pp60^{c\text{-}src}$ expression levels were determined from immunoprecipitates of cells with monoclo-

R. Azarnia and W. R. Loewenstein, Department of Physiology and Biophysics, University of Miami School of Medicine, Miami, FL 33136.
S. Reddy, T. E. Kmiecik, D. Shalloway, Department of Molecular Cell Biology, Pennsylvania State University, University Park, PA 16802.

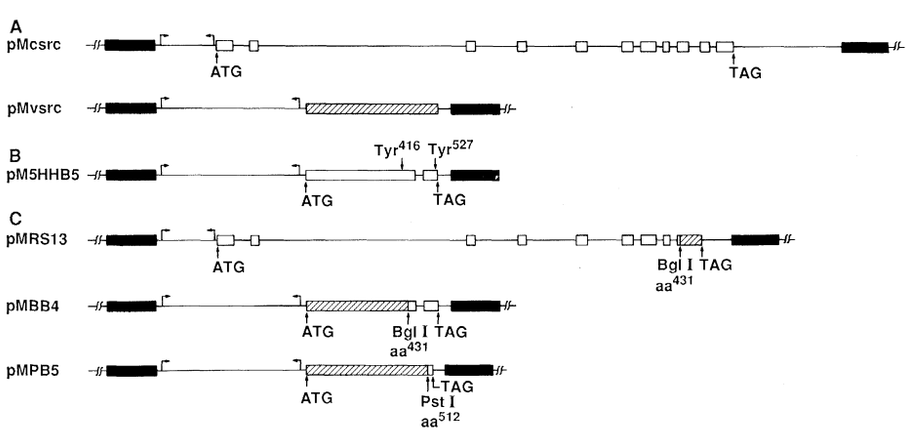

Fig. 1. The c-*src* and v-*src* expression plasmids. The plasmids contain the chicken c-*src*, v-*src*, mutant, and chimeric *src* genes ligated to transcriptional enhancers, promoters, and polyadenylation signals provided by flanking Moloney murine leukemia virus long terminal repeats (filled boxes) from the vector pEVX (*23*). The locations of Moloney splice donors and first *src* splice acceptors are denoted by bent arrows. Coding regions are indicated by open (c-*src*) or hatched boxes (v-*src*), and the locations of the initiating (ATG) and terminating (TAG) codons are marked. Only the functionally relevant eukaryotic regions of the plasmids are shown (*11, 20*). (**A**) pMcsrc, the plasmid used in the experiments on c-*src* overexpression, and the structurally similar v-*src* expression plasmid pMvsrc; (**B**) pM5HHB5, the plasmid used for site-directed mutagenesis. The Tyr → Phe codon exchanges were produced at amino acids 416, 527, or both, generating plasmids pcsrc416, pcsrc527, and pc416 527 by replacing the small fragments containing the codons to be exchanged with DNA fragments containing the appropriate mutations. These mutated plasmids have the same restriction map as pM5HHB5. (**C**) Plasmids pMRS13 and pMBB4 are mirror-image chimeric constructions with junctions at site Bgl I at amino acid (aa) codon 431. pMPB5 is similar to pMBB4, except that the junction is at the Pst I site at amino acid 512.

nal antibody mAb327 which recognizes both chicken and mouse $pp60^{c\text{-}src}$ (*6*). Cells were individually microinjected with Lucifer Yellow (443 daltons) or with glutamic acid labeled with lissamine rhodamine B (LRB-Glu; 688 daltons) and the cell-to-cell flow of these fluorescent tracers was video-recorded for analysis. The incidence of permeable interfaces, that is, the proportion of the first-order neighbors of the injected cell to which the tracers were transferred within 20 seconds, for Lucifer Yellow and 5 minutes for LRB-Glu served as index of junctional permeability (*7*). To facilitate comparisons between experiments, the incidence values were normalized with respect to those of the controls.

For the experiments on gene overexpression, we used three clones of c-*src*–transfected cells [NIH(pMcsrc)] in which $pp60^{c\text{-}src}$ was elevated 10 to 20 times relative to the untransfected controls (*8*). All three had strikingly low capacities of junctional transfer. Whereas the control cells passed the fluorescent tracers frequently and extensively to first-order and higher order neighbors, the overexpressor cells passed them rarely and only to first-order neighbors (Fig. 2). In the three clones the incidence of interfaces permeable to Lucifer Yellow was reduced by 57, 64, and 73%, the clone with the highest $pp60^{c\text{-}src}$ level exhibiting the greatest reduction (Table 1).

The permeability of nonjunctional cell membranes was not affected by the c-*src* overexpression, as shown by measurement of the rates of tracer loss from the cells. Both overexpressor and control cells exhibited negligible losses over periods of 10 minutes (Fig. 2, C and D). Thus, the decrease in junctional transfer represents a decrease in junctional permeability.

Using plasmids of analogous construction (Fig. 1), we compared the effect of c-*src* with that of the viral *src* gene (*9*), which encodes a more potent tyrosine protein kinase ($pp60^{v\text{-}src}$) (*2*). Cells containing the viral gene [NIH(pMvsrc)] showed higher tyrosine phosphorylation levels and lower junctional permeabilities than cells containing c-*src* (Table 1).

The c-*src* ability to down-regulate communication was enhanced when the gene was endowed with the carboxyl-terminal coding region of the viral gene. Such c-*src* chimeras v-*src* (Fig. 1) induced losses of communication comparable to those induced by the full viral gene, even at low gene expression (Table 2). Conversely, when the viral gene was furnished with the c-*src* carboxyl-terminal coding region, its down-regulatory action was inhibited. In the five cell clones containing such v-*src*/c-*src* chimeras [including mirror images (pMBB4) of the preceding ones] the junctional permeabilities were not significantly different from the controls (Table 2).

These results indicated that the carboxyl-terminal region is a determinant of the regulation of communication by *src*. Next we examined the effect of point mutation in that region, using a site-directed mutant c-*src* vector (pcsrc527) (Fig. 1) that encodes a substitution of Phe (which cannot be phosphorylated) for Tyr^{527}. Several lines of evidence indicate that Tyr^{527} phosphorylation, which occurs in vivo (*10*), inhibits the enzyme and transforming activity of $pp60^{c\text{-}src}$ (*11, 12*). Cells containing this mutant gene had much lower junctional permeabilities than controls containing the unmodified c-*src* vector (pM5HHB5), even though $pp60^{c\text{-}src}$ expression was lower than in these controls (Table 3) (*13*). The junctional permeability also was much lower than that of controls containing *neo* alone (pSV2neo). The effect of the Tyr^{527} mutation was nearly as pronounced as that of the c-*src*/v-*src* chimeras; most cells exhibited no junctional transfer at all (*14*). The mutation evidently had caused a reduction of junctional permeability on its own, which was associated with the rise in transforming activity of $pp60^{c\text{-}src}$ (*11*).

Further, we examined the effect of Phe substitution for Tyr^{416}, the site that becomes stably phosphorylated in vivo upon mutation of Tyr^{527} (*11*) and transiently phosphorylated upon c-*src* overexpression (*15*). This mutation inhibited the ability of c-*src* to down-regulate communication, even when the Tyr^{527} mutation was present. Cells containing genes with such a mutation in addition to that at Tyr^{527} (pcsrc416·527) had junctional permeabilities similar to those of the controls (pM5HHB5); and cells containing genes with the single Tyr^{416} mutation (pcsrc416), and expressing $pp60^{c\text{-}src}$ at a level ten times the endogenous one, showed junctional permeabilities not significantly different from the controls (pSV2neo) containing only endogenous

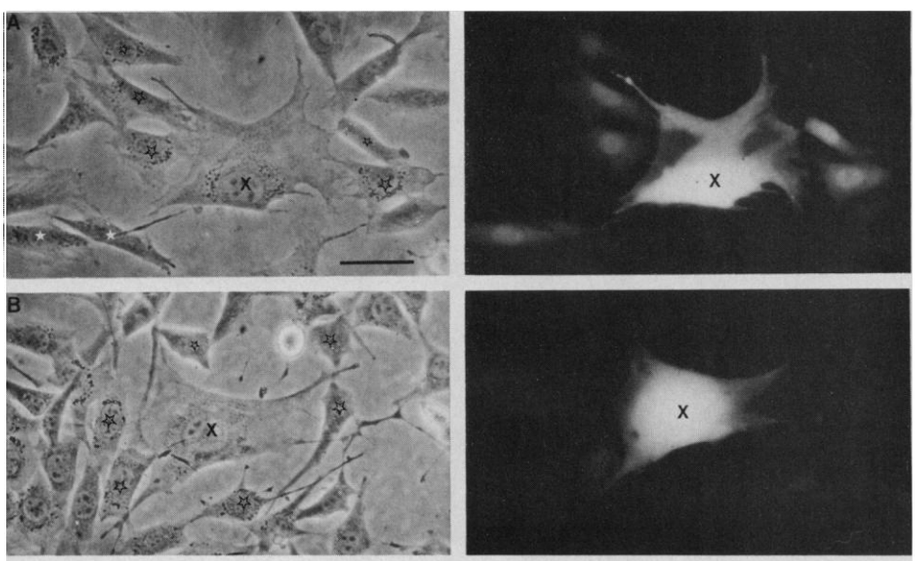

Fig. 2. Reduced junctional permeability in cells overexpressing c-*src*. Photomicrographs of sample microinjection of Lucifer Yellow into NIH 3T3 cells shown in phase contrast (left) and in fluorescence mode (right) after injection. Injected cell is marked by X; its first-order neighbors are marked by stars. (**A**) Control cells (untransfected NIH 3T3). The fluorescent tracer has spread to all of the seven first-order neighbors. (**B**) Cells with elevated c-*src* expression (20-fold) [NIH(pMcsrc/foc)B]; the tracer has spread to one out of six first-order neighbors. Calibration, 50 μm. Rates of Lucifer Yellow fluorescence loss from (**C**) a control and (**D**) an overexpressor cell. Chart records of the intracellular fluorescence intensity excited with intermittent light pulses. Cells were cultured in DMEM (Dulbecco modification of Eagle minimal essential medium) supplemented with 5% calf serum (Gibco) on 35-mm plastic dishes at 37°C in an atmosphere of 95% air and 5% CO_2. During the determinations of junctional transfer (limited to periods of 20 minutes) and of fluorescence loss, the cells were at 30° to 32°C, exposed to room air. Rates of fluorescence loss were measured on cells without neighbors (very sparse cultures) by means of a photodiode onto which the image of a spot of the cell was projected through the microscope (*24*). Excitation parameters, 560 nm; pulses of 5-second duration, one per minute.

pp60$^{c\text{-}src}$ (Table 3). This suggests that phosphorylation of Tyr^{416} is necessary for c-*src*–induced down-regulation of communication.

In conclusion, down-regulation of communication can be induced by an increase in c-*src* transcription rate or by modifications enhancing the product's transforming activity. The modification of a single codon, Tyr^{527}, can activate this down-regulation and modification of Tyr^{416} abolishes it. Tyr^{527} appears to provide negative control, which is switched off by dephosphorylation of this site and associated phosphorylation of Tyr^{416}.

In pondering the physiological role of this regulatory action, we are drawn at once to development and growth where a body of evidence indicates that junctional communication is important (*16*). The pp60$^{c\text{-}src}$ is known to undergo changes in expression level, structure, and enzyme activity during embryonic development (*17*); and we have shown (*18*) that the down-regulation of communication by c-*src* overexpression correlates with increased saturation density of cell growth in vitro. It remains to be seen whether the junctional channel itself (*19*) or a channel regulator is the phosphorylation target.

Table 1. Junctional communication of c-*src* overexpressor cells.

Cells	pp60^{src} expression level*	In vivo phosphotyrosine†	Permeable interfaces‡	
			Lucifer Yellow	LRB-Glu
NIH 3T3(control)	1	1.0	1.0 ± 0.08 (32)	1.0 ± 0.03 (20)
NIH(pMcsrc/cos)A	10	1.0	0.43 ± 0.08 (38)	
NIH(pMcsrc/foc)A	14		0.36 ± 0.03 (50)	
NIH(pMcsrc/foc)B	20	2.5	0.27 ± 0.05 (55)	0.31 ± 0.01 (40)
NIH(pMvsrc/cos)A	2	3.4	0.05 ± 0.03 (50)	
NIH(pMvsrc/foc)A	2	5.3	0.11 ± 0.05 (16)	0.09 ± 0.01 (40)

*Relative steady-state pp60^{src} expression was determined from immunoprecipitates (mAb327) of cell lysates labeled to equilibrium with [^{35}S]methionine for 48 hours, normalized to the expression level of NIH 3T3 control cells (*20*). Standard fractional error $< \times\div 1.2$; the low endogenous level of NIH 3T3 may have additional background subtraction error. †Relative phosphotyrosine in vivo from ^{32}P-labeled phosphoamino acid analysis of total cell proteins (*21*). Labeled phosphoamino acids were separated by two-dimensional electrophoresis (*22*), and the proportion of radioactivity in phosphotyrosine was calculated as a fraction of radioactivity in all cell phosphorylhydroxyamino acids and normalized to the phosphotyrosine fraction in NIH 3T3 controls (0.015%). ‡Relative incidence of interfaces permeable to Lucifer Yellow or LRB-Glu. The values are arithmetic means ± SE of the incidences determined on individual cells, normalized to the mean incidence of NIH 3T3 controls (the absolute means of the controls were 0.37 ± 0.03, Lucifer Yellow; 0.86 ± 0.03, LRB-Glu). The number of indepedent measurements, that is, the number of cells injected, is given in parentheses. Each incidence value of the *src*-transfected cells differed from controls at a significance level $P < 0.00005$ (*t* test with Bonferroni's correction for multiple comparisons).

Table 2. Junctional communication of cells expressing *src* chimeras.

Cells	pp60^{src} expression level*	Permeable interfaces†	*P*‡
Control			
NIH 3T3	1	1.0 ± 0.08 (32)	
c-*src*/v-*src*			
NIH(pMRS13/foc)C	2	0.13 ± 0.06 (50)	0.000007
NIH(pMRS13/foc)D	2	0.04 ± 0.02 (50)	0.000007
v-*src*/c-*src*			
NIH(pMBB4/foc)E	3	0.8 ± 0.2 (50)	ns
NIH(pMBB4/foc)I	6	0.9 ± 0.2 (32)	ns
NIH(pMBB4/foc)H	2	0.5 ± 0.2 (50)	ns (0.07)
NIH(pMPB5/foc)B	7	1.3 ± 0.2 (50)	ns
NIH(pMPB5/foc)E	1	1.0 ± 0.2 (50)	ns

*Values are geometric means of two measurements; the fractional standard errors ranged $\times\div$ 1.06 to 1.3; methods in Table 1. †Probings with Lucifer Yellow. Arithmetic means ± SE; in parentheses, the number of cells injected. ‡Statistical significance level of the difference between the various mean incidence values of permeable interfaces and the mean value of the controls (*t* test with Bonferroni's correction); ns, not significant.

REFERENCES AND NOTES

1. D. Stehelin, H. E. Varmus, J. M. Bishop, P. K. Vogt, *Nature (London)* **260**, 170 (1976).
2. T. Hunter and J. Cooper, *Annu. Rev. Biochem.* **54**, 897 (1985).
3. R. Azarnia and W. R. Loewenstein, *Mol. Cell Biol.* 7, 946 (1987).
4. S. A. Courtneidge and A. E. Smith, *Nature (London)* **303**, 435 (1983); J. B. Bolen, C. J. Thiele, M. A. Israel, L. A. Lipsich, J. S. Brugge, *Cell* **38**, 767 (1984).
5. Cells were transfected by the calcium phosphate coprecipitation technique, with glycerol (15%) as adjuvant; N. G. Copeland and G. M. Cooper, *Cell* **16**, 347 (1979). The *src*:*Eco-gpt* and *src*:*neo* ratios were equimolar and 6:1, respectively. The mutants were selected as described by R. C. Mulligan and P. Berg [*Science* **209**, 1422 (1980)] and P. J. Southern and P. Berg [*J. Mol. Appl. Genet.* **1**, 327 (1982)].
6. L. A. Lipsich, A. J. Lewis, J. S. Brugge, *J. Virol.* **48**, 352 (1983).
7. At these intervals the incidence values were well below 1.0, providing sensitive, nonsaturated permeability indices, as shown before by measurements of junctional transfer rates in 3T3 cell pairs (*24*) and corroborated for NIH 3T3 here. In all cases analyzed, first-order neighbors were clearly distinguished in phase contrast, permitting accurate counting of cell interfaces. Transfer was determined at cell densities of 2 to 12 (10^4 cells per square centimeter), where the incidence of permeable interfaces was independent of density. This working range was established in experiments comparing, for each given cell line, the mean incidence at three to

Table 3. Tyr^{527} and Tyr^{416} mutants.

Cells	c-*src* expression or mutation	pp60^{src} expression level*	Specific enzyme activity†	Permeable interfaces‡	P_1§	P_2§
NIH 3T3	Endogenous pp60$^{c\text{-}src}$	1		1.00 ± 0.08 (32)	ns	0.04
NIH(pSV2neo)	Endogenous pp60$^{c\text{-}src}$	1		0.92 ± 0.08 (50)		0.02
NIH(pM5HHB5/*neo*)	Overexpressed pp60$^{c\text{-}src}$	13	1	0.73 ± 0.08 (50)	0.02	
NIH(pcsrc527/*neo*)	Tyr^{527} → Phe^{527}	8	13	0.28 ± 0.05 (82)	0.000005	0.00004
NIH(pcsrc416/*neo*)	Tyr^{416} → Phe^{416}	10	1	0.93 ± 0.04 (30)	ns	ns
NIH(pcsrc416·527/*neo*)	Tyr^{527} → Phe^{527}; Tyr^{416} → Phe^{416}	20	7	0.66 ± 0.08 (59)	0.04	ns

*Geometric-mean values; the fractional standard errors ranged $\times\div$ 1.03 to 1.2; The low NIH 3T3 and NIH(pSV2neo) expression level may have additional background subtraction error. The methods were as in Table 1, but the [^{35}S]methionine labeling for pp60^{src} was 40 to 44 hours. Values for pp60^{src} expression are not comparable with those of Tables 1 and 2 (*13*). †In vitro specific tyrosine kinase activity was determined by incubating monoclonal antibody-bound [^{35}S]methionine-labeled pp60^{src} with [γ-^{32}P]ATP and comparing the amount of phosphate transferred to α-enolase with the amount of pp60^{src} present as determined by double-channel scintillation counting (*11*). Values are geometric means of three measurements; the fractional errors ranged $\times\div$ 1.5 to 1.6. ‡Arithmetic means ± SE; in parentheses, the number of cells injected. §P_1 and P_2 are the statistical significance levels of the differences between the various mean incidence values of permeable interfaces and the mean value of the NIH(pSV2neo) controls or the NIH(pMHHB5/*neo*) controls, respectively (*t* test with Bonferroni's correction).

four density points (12 to 41 injections per point).
8. P. J. Johnson, P. M. Coussens, A. V. Danko, D. Shalloway, *Mol. Cell Biol.* **5**, 1073 (1985).
9. M. M. Atkinson, A. S. Menko, R. G. Johnson, J. R. Sheppard, J. D. Sheridan, *J. Cell Biol.* **91**, 573 (1981); R. Azarnia and W. R. Loewenstein, *J. Membrane Biol.* **82**, 191, 207 (1984).
10. J. A. Cooper *et al.*, *Science* **231**, 1431 (1986).
11. T. E. Kmiecik and D. Shalloway, *Cell* **49**, 65 (1987).
12. H. Piwnica-Worms, K. B. Saunders, T. M. Roberts, A. E. Smith, S. H. Cheng, *ibid.*, p. 75; C. A. Cartwright, W. Eckhart, S. Simon, P. L. Kaplan, *ibid.*, p. 83.
13. The $pp60^{c\text{-}src}$ expression levels here were from experiments independent of those in Tables 1 and 2. Because the low endogenous expression level in NIH 3T3 was not measurable to high accuracy, it does not serve as an external standard, and thus the $pp60^{c\text{-}src}$ expression levels of Table 3 are not comparable with those of Tables 1 and 2; the permeable-interface data, however, are comparable.
14. As in the case of c-*src* overexpression, the expression of Tyr^{527} mutants or c-*src*/v-*src* chimeras did not affect nonjunctional membrane permeability; the rates of loss of Lucifer Yellow were negligible and not different from controls (six photometric measurements as in Fig. 2, C and D, were performed for each condition).
15. T. E. Kmiecik, P. J. Johnson, D. Shalloway, in preparation.
16. W. R. Loewenstein, *Cell* **48**, 725 (1987).
17. L. K. Sorge, B. T. Levy, T. M. Gilmer, P. F. Maness, *Cancer Cells* **1**, 117 (1984); J. S. Brugge *et al.*, *Nature (London)* **316**, 554 (1985); J. S. Brugge *et al.*, *Genes Dev.* **1**, 287 (1987); R. Martinez, B. Mathey-Prevot, A. Bernards, D. Baltimore, *Science* **237**, 411 (1987).
18. R. Azarnia, S. Reddy, T. E. Kmiecik, D. Shalloway, W. R. Loewenstein, in preparation.
19. A subunit of gap-junction protein contains tyrosines in the cytoplasmic domain with the consensus sequence for phosphorylation [D. L. Paul, *J. Cell Biol.* **103**, 123 (1986); N. M. Kumar and N. B. Gilula, *J. Cell Biol.* **103**, 767 (1986)].
20. P. J. Johnson, P. M. Coussens, A. V. Danko, D. Shalloway, *Mol. Cell Biol.* **5**, 1073 (1985); S. Reddy *et al.*, in preparation.
21. P. M. Coussens, J. A. Cooper, T. Hunter, D. Shalloway, *Mol. Cell Biol.* **5**, 2573 (1985).
22. J. A. Cooper and T. Hunter, *ibid.* **1**, 165 (1981).
23. M. Kriegler, C. F. Perez, M. Botchan, *Cell* **38**, 483 (1984).
24. J. L. Flagg-Newton, G. Dahl, W. R. Loewenstein, *J. Membrane Biol.* **63**, 105 (1981).
25. We thank Joan Brugge for antibody mAb327. Supported by research grants CA-14464 and CA-32317 from the National Cancer Institute, National Institutes of Health.
23 April 1987; accepted 15 December 1987

Suppression of Macrophage Activation and T-Lymphocyte Function in Hypoprolactinemic Mice

EDWARD W. BERNTON,* MONTE S. MELTZER, JOHN W. HOLADAY

The effects of prolactin on lactation and reproductive organs are well known. However, the other possible target organs and physiological consequences of altered levels of circulating prolactin remain poorly understood. In this study, mice were treated with bromocryptine, a dopamine receptor agonist that inhibits pituitary prolactin secretion. Bromocryptine treatment prevented T-cell–dependent induction of macrophage tumoricidal activity after the intraperitoneal injection of *Listeria monocytogenes* or *Mycobacterium bovis*. Coincident treatment with ovine prolactin reversed this effect. Of the multiple events leading to macrophage activation in vivo, the production by T-lymphocytes of γ-interferon was the most impaired in bromocryptine-treated mice. Lymphocyte proliferation after stimulation with mitogens in vitro was also depressed in spleens of bromocryptine-treated mice, and coadministration of prolactin also reversed this effect. Bromocryptine treatment also reduced the number of deaths resulting from inoculation of mice with *Listeria*; exogenous prolactin significantly reversed this effect. The critical influence of pituitary prolactin release on maintenance of lymphocyte function and on lymphokine-dependent macrophage activation suggests that, in mice, lymphocytes are an important target tissue for circulating prolactin.

A NUMBER OF REGULATORY INTERactions among the central nervous system (CNS), the neuroendocrine axis, and the immune system have recently been described. Endocrine and autocrine mediators and receptors shared in common by the immune and endocrine systems may explain changes in immune function in response to environmental stimuli perceived by the CNS (*1*). Although high levels of endogenous (adrenal) or exogenous corticosteroids can suppress many immune responses, immunosuppression induced in rats by repeated periods of tail-shock persists after adrenalectomy (*2*). Such data suggest that other neural and endocrine mechanisms under CNS control may have immunomodulatory roles beyond the activation of the pituitary-adrenocortical axis as a result of stress.

Pituitary prolactin secretion is regulated not only by reproductive hormones, but also by CNS pathways affected by both acute and chronic stressors as well as by many CNS-active drugs, such as opiates and aminergic agonists and antagonists (*3*). Several lines of evidence indicate that prolactin (PRL) may be an important immunoregulatory hormone. In rats, both hypophysectomy and treatment with the dopamine agonist bromocryptine inhibit the development of delayed cutaneous hypersensitivity, experimental allergic encephalitis, or adjuvant-induced arthritis; treatment with exogenous PRL reverses these immunosuppressive effects (*4*). Cyclosporine, an immunosuppressive fungal peptide that inhibits T-cell function, inhibits PRL binding to lymphocytes (*5, 6*). Two hypopituitary strains of mice, the Ames and Snell dwarfs, develop impaired cellular immunity and hypotrophic thymuses after weaning; this immunodeficiency is prevented by injections of milk, a PRL source (*7*). However, the mechanisms mediating immunosuppression in hypoprolactinemic animals have not been elucidated.

We therefore examined the T cell–dependent induction of activated, tumoricidal macrophages in mice infected with either *Mycobacterium bovis* (strain BCG) or *Listeria monocytogenes* (LM), or inoculated with killed *Proprionibacterium acnes*. Bromocryptine, a dopamine type 2 (DA-2) agonist, was used to continuously suppress serum PRL to less than 2.0 ng/ml (*8*). Injections of bromocryptine on days −1 to 3 before and after inoculation with either BCG, LM, or *P. acnes* on day 0 prevented induction of tumoricidal macrophages (Fig. 1). However, the timing of DA-2 agonist administration was critical. Daily bromocryptine treatment either on days 0 and 1 or on days 4 through 7 did not alter macrophage activation. This time course indicated that one or more early steps in the pathway of macrophage activation in vivo were blocked by DA-2 agonist administration.

Since DA-2 agonists exert physiological effects other than the inhibition of PRL release, we examined whether exogenous PRL could reverse the effects of bromocryptine treatment. Simultaneous daily intraperitoneal injection of ovine PRL (100 μg/day) (*9*) restored to normal the induction of tumoricidal macrophages during BCG or LM infection in bromocryptine-treated ani-

E. W. Bernton and J. W. Holaday, Neuropharmacology Branch, Department of Medical Neurosciences, Division of Neuropsychiatry, Walter Reed Army Institute of Research, Washington, DC 20307.
M. S. Meltzer, Department of Immunology, Division of Communicable Disease and Immunology, Walter Reed Army Institute of Research, Washington, DC 20307.

*To whom correspondence should be addressed.